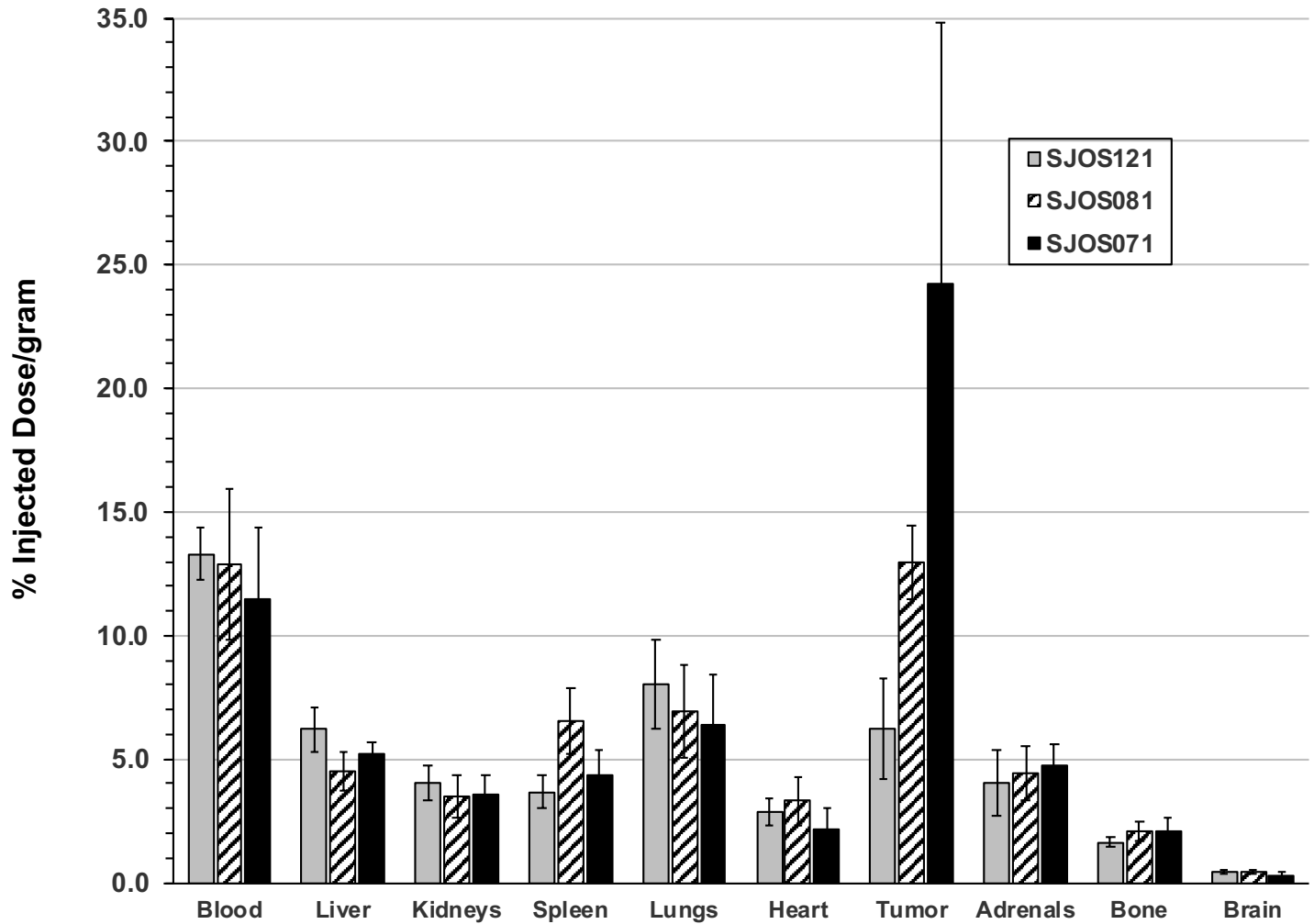


## Supplementary Data

### Positron Emission Tomography Detects *In Vivo* Expression of Disialoganglioside GD2 in Mouse Models of Primary and Metastatic Osteosarcoma

Elizabeth R. Butch<sup>1</sup>, Paul E. Mead<sup>2</sup>, Victor Amador-Diaz<sup>1</sup>, Heather Tillman<sup>2</sup>, Elizabeth Stewart<sup>3</sup>, Jitendra K. Mishra<sup>1‡</sup>, Jieun Kim<sup>6</sup>, Armita Bahrami<sup>2</sup>, Jason L.J. Dearling<sup>7,8</sup>, Alan B. Packard<sup>7,8</sup>, Shana V. Stoddard<sup>1†</sup>, Amy L. Vāvere<sup>1</sup>, Yuanyuan Han<sup>4</sup>, Barry L. Shulkin<sup>1</sup> and Scott E. Snyder<sup>\*1,5</sup>



**Figure S1.** *Ex vivo* biodistribution data for PDXs SJOS071, SJOS081 and SJOS121. Osteosarcoma tumor-bearing nude (NCr-*Foxn1<sup>nu</sup>*) mice (SJOS071, n = 5; SJOS081, n = 9; SJOS121, n = 5) were anesthetized (1.5-2% isoflurane) and injected (*r.o.*) with 75  $\mu$ Ci (2.4-3.0 MBq, 100 $\mu$ L) of [<sup>64</sup>Cu]Cu-Bn-NOTA-hu14.18K322A formulated in isotonic saline. At 48 h post-injection of radiotracer, animals were anesthetized and euthanized by decapitation. Tissues were dissected, weighed and counted for radioactivity. Data were calculated as the percentage of injected dose per gram of wet tissue (mean  $\pm$  standard deviation; %ID/g). The <sup>64</sup>Cu concentration in non-target tissues was consistent across all groups whereas tumor <sup>64</sup>Cu concentration was proportional to GD2 expression measured *in vitro* by flow cytometry.

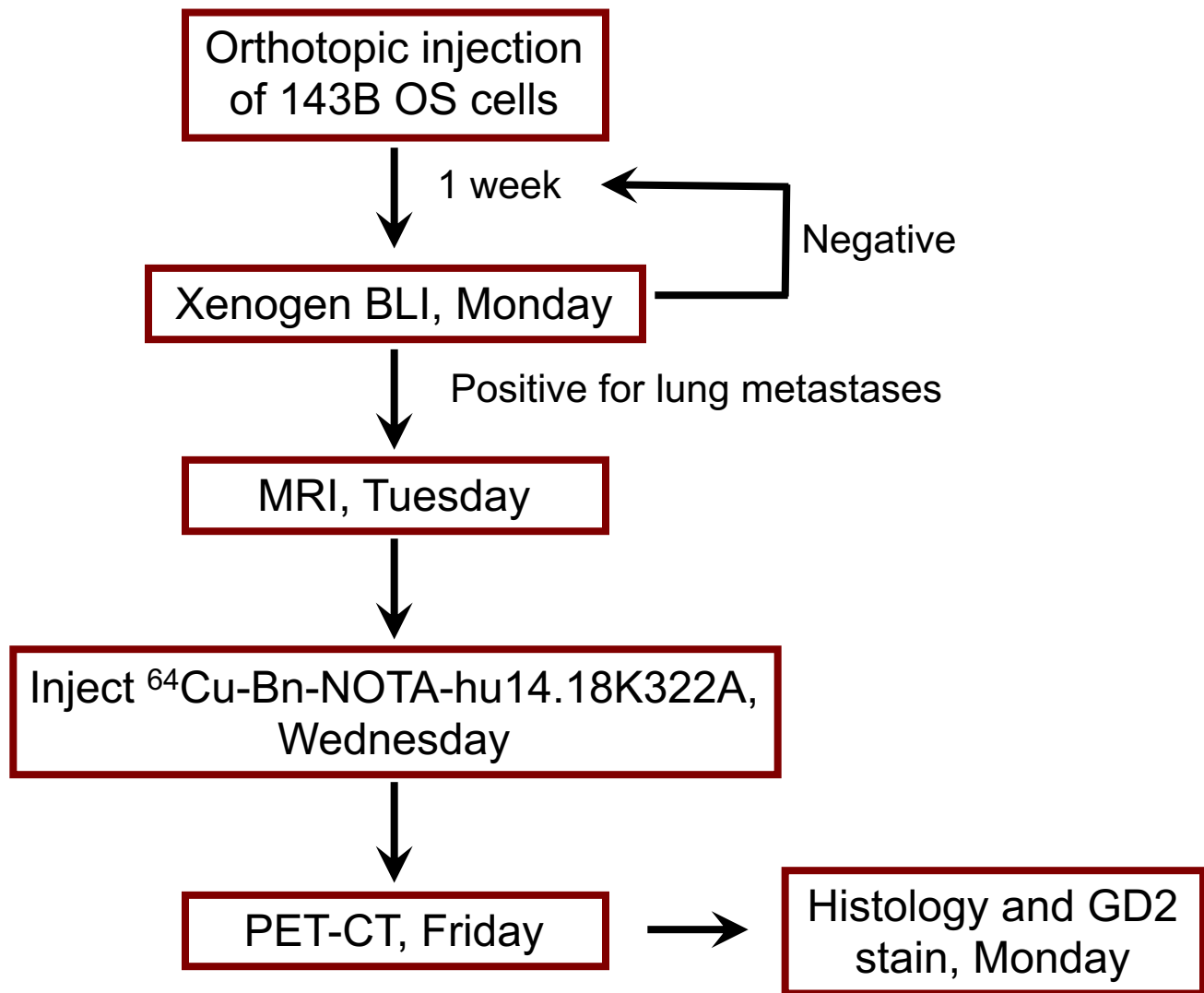


**Figure S2.** Multimodality imaging protocol. Tumor-bearing mice were subjected to weekly imaging sessions starting Monday with injection of *D*-luciferin followed by bioluminescence imaging (BLI) of YFP-luciferase-labeled 143B cells to monitor primary tumor engraftment as well as the development of metastatic disease. Animals proven positive for lung metastases on BLI were imaged Tuesday using MRI, and then Wednesday were injected *r.o.* with 65-80  $\mu\text{Ci}$  (2.4-3.0 MBq) of [<sup>64</sup>Cu]Cu-Bn-NOTA-hu14.18K322A. At 48 h post-injection of radiotracer, animals were imaged by PET-CT (Friday). After allowing an additional 72 h for radioactivity decay, animals were euthanized and tissues of interest were dissected and submitted for sectioning and histologic analysis.

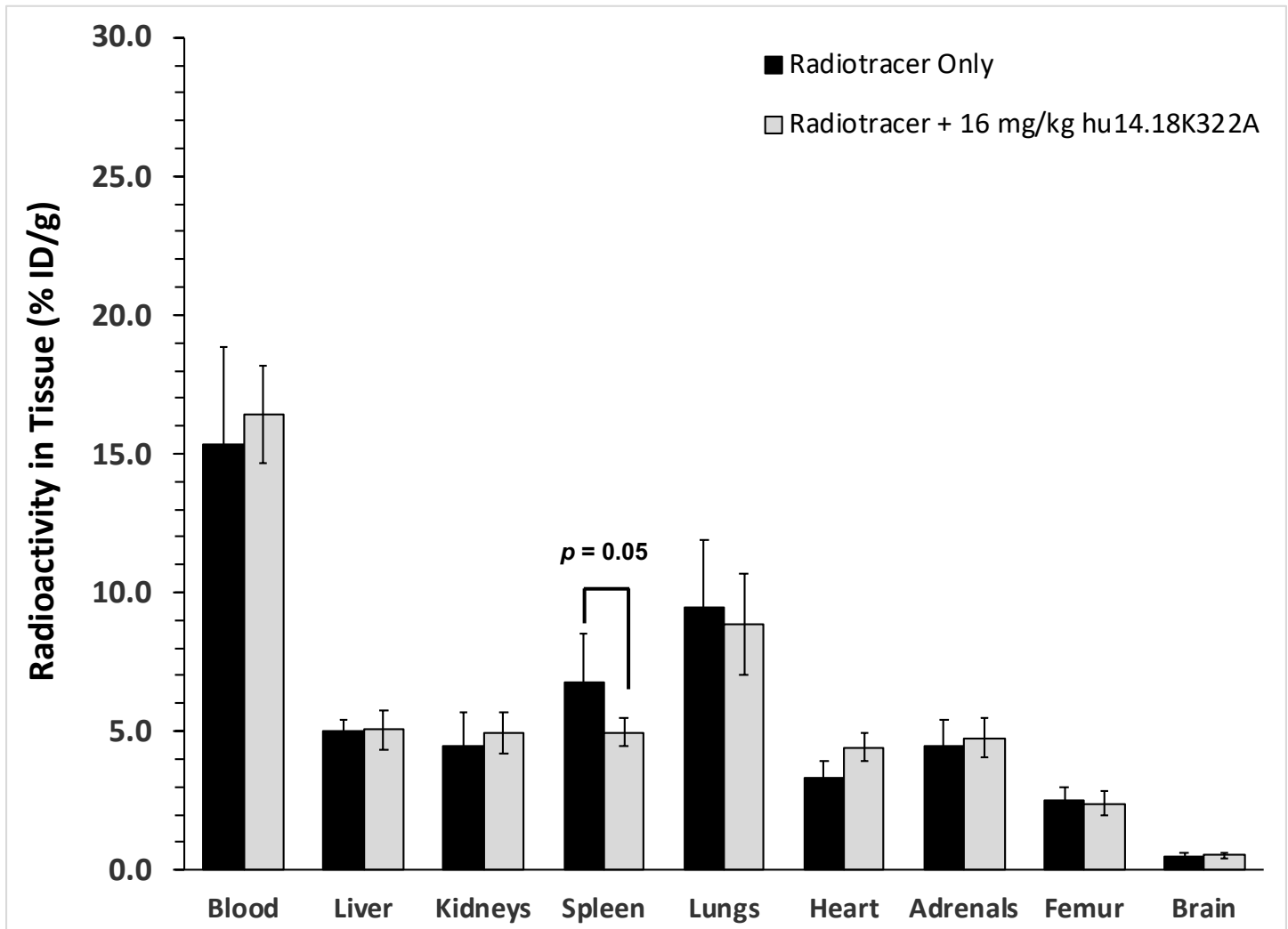


**Figure S3.** Biodistribution of [ $^{64}\text{Cu}$ ]Cu-Bn-NOTA-hu14.18K322A in non-tumored nude mice co-injected with a therapeutic dose of unmodified hu14.18K322A. Female athymic NCr-*Foxn1*<sup>nu</sup> nude mice (n = 5-8 per group) were injected (*r.o.*) with 75  $\mu\text{Ci}$  (2.4-3.0 MBq, 100 $\mu\text{L}$ ) of [ $^{64}\text{Cu}$ ]Cu-Bn-NOTA-hu14.18K322A formulated in isotonic saline either alone or co-injected with 16 mg/kg of unmodified hu14.18K322A. This dose of hu14.18K322A in mice was calculated by allometric scaling of the human pharmacologically effective dose of 40 mg/kg. At 48 h post injection, animals were anesthetized and euthanized by decapitation. Tissues were dissected, weighed and counted for radioactivity. Data were calculated as the percentage of injected dose per gram of wet tissue (%ID/g). No significant difference in blood radiotracer concentration ( $p=0.57$ ) at 48 hours post-injection was observed between mice injected with radiotracer only and those co-injected with radiotracer plus the pharmacological dose of unmodified hu14.18K322A, indicating no specific binding of radiotracer in the blood. In fact, none of the non-target organs showed any significant difference between these groups with the exception of spleen ( $p=0.05$ ). The decrease in spleen accumulation is likely due to competition of the unlabeled antibody for accumulation in spleen *via* interaction with non-specific IgG clearance mechanisms (Cataldi M, Vigliotti C, Mosca T, Cammarota, MR and Capone D. Review: Emerging Role of the Spleen in the Pharmacokinetics of Monoclonal Antibodies, Nanoparticles and Exosomes. *Int J Mol Sci* 2017;18:1249).

Animal #	BLI	MRI	PET			Histology		
			PET(max)	PET(mean)	Volume (mm <sup>3</sup> )	Primary tumor	Lung <sup>a</sup>	Comments
1	-	-	-	-	-	+	+	Micro-metastases
2	+	-	-	-	-	+	+	Micro-metastases
3	+	+	20.5 <sup>b</sup>	10.5	72	+	+	Multifocal metastases present
			19.2	11.3	29.3			
4	-	-	-	-	-	-	-	No primary or metastatic xenograft present.
5	+	+	(c)	(c)	~1 <sup>d</sup>	+	+	Lung metastases present
6	+	+	9.8	6.3	12.4	+	+	Lung metastases present
7	-	-	-	-	-	+	+	Individualized lung tumor cells
8	-	-	-	-	-	+	-	Lung tumor cells not detected

**Table S1.** Summary of multi-modality imaging study on a mouse model of osteosarcoma metastatic to the lung. Animal 4 showed no evidence of successful engraftment at the primary or metastatic sites. Animals 1, 7 and 8 displayed no lung involvement by luciferase imaging or MRI, so [<sup>64</sup>Cu]Cu-Bn-NOTA-hu14.18K322A PET imaging was not performed. Presence of the primary engraftment was confirmed by histology in all three of these animals and individualized tumor cells were identified in the lungs of animals 1 and 7. Animal 2 showed lung metastases by BLI which was confirmed as micro-metastasis on histology. MRI and PET were both negative for this animal. Animal 5 was positive for lung involvement on BLI and MRI, but lesions were too small (~1 mm<sup>3</sup>) to be distinguished from background on the PET images. Similarly, animal 6 showed a small 12 mm<sup>3</sup> site of lung disease that was visible on PET but <sup>64</sup>Cu concentration in this site was not significantly above the blood levels in the pulmonary vessels. Detailed imaging results for animal 3 are presented in Figure 4 and the corresponding histology results in Figure 5.

- a) All metastatic tumor cells have a morphology consistent with the primary tumor phenotype
- b) Multiple lung lesions detected by PET for this animal
- c) Lesion not discernable from normal lung background by PET
- d) Tumor region of interest volume was based on MRI; not visible on CT or PET